

# Mechanism of the Membrane Interaction of Polynuclear Platinum Anticancer Agents. Implications for Cellular Uptake<sup>†</sup>

Qin Liu,<sup>‡</sup> Yun Qu,<sup>‡</sup> Rik Van Antwerpen,<sup>§</sup> and Nicholas Farrell<sup>\*,‡</sup>

Department of Chemistry, Virginia Commonwealth University, Richmond, Virginia 23284-2006, and  
Biochemistry Department, Virginia Commonwealth University, Richmond, Virginia 23298

Received December 9, 2005; Revised Manuscript Received February 7, 2006

**ABSTRACT:** The interaction between phospholipids and polynuclear platinum drugs was studied as a mechanism model for cellular uptake of anticancer drugs. The interaction was studied by differential scanning calorimetry (DSC), <sup>31</sup>P nuclear magnetic resonance spectroscopy (NMR), inductively coupled plasma optical emission spectroscopy (ICP-OES), and electrospray ionization mass spectrometry (ESI-MS). The transition temperature, enthalpy, and entropy of negatively charged phospholipids DPPS, DPPA, and DPPG were changed upon reaction with the trinuclear platinum complex [*trans*-PtCl(NH<sub>3</sub>)<sub>2</sub>]<sub>2</sub>μ-Pt(NH<sub>3</sub>)<sub>2</sub>{H<sub>2</sub>N(CH<sub>2</sub>)<sub>6</sub>NH<sub>2</sub>}(NO<sub>3</sub>)<sub>4</sub> (**I**, BBR3464) and the dinuclear analogue [*trans*-PtCl(NH<sub>3</sub>)<sub>2</sub>]<sub>2</sub>μ-{(NH<sub>2</sub>)(CH<sub>2</sub>)<sub>3</sub>NH<sub>2</sub>(CH<sub>2</sub>)<sub>4</sub>(NH<sub>2</sub>)}Cl<sub>3</sub> (**II**, BBR3571). This suggests that these platinum complexes interacted not only with the phosphate headgroup but also with the region of the fatty acid tail of liposomes and finally changed the fluidity of the membrane. Both noncovalent (presumably electrostatic and hydrogen bonding) and covalent interactions were involved in the reactions of the negatively charged phospholipids DPPA, DPPS, and DPPG with the highly positively charged platinum complexes. In contrast, few differences were seen for the zwitterionic phospholipids DPPC and DPPE. The binding ratio of BBR3464 to DPPA liposomes was higher than the ratio of BBR3464 to DPPS liposomes, and similar differences were seen for BBR3571. The binding ratios of the platinum complexes to negatively charged phospholipids DPPA, DPPS, and DPPG were slightly lower in a 100 mM chloride solution than in a chloride-free solution. The binding of BBR3464 and BBR3571 with the liposomes was significantly stronger than that with *cis*-[PtCl<sub>2</sub>(NH<sub>3</sub>)<sub>2</sub>], cisplatin. ESI-MS confirmed that the products of the incubation of BBR3464 with DPPA and DPPS correspond to chloride displacement and formation of [Pt<sub>3</sub>(NH<sub>3</sub>)<sub>6</sub>{NH<sub>2</sub>(CH<sub>2</sub>)<sub>6</sub>NH<sub>2</sub>}(DPPA)<sub>2</sub>]<sup>2+</sup> (**1**) and [Pt<sub>3</sub>(NH<sub>3</sub>)<sub>6</sub>{NH<sub>2</sub>(CH<sub>2</sub>)<sub>6</sub>NH<sub>2</sub>}(DPPS)<sub>2</sub>]<sup>2+</sup> (**2**), respectively. Similar observations were made for BBR3571. <sup>31</sup>P NMR spectra confirmed that the site of binding for DPPA was the phosphate oxygen, whereas for DPPS, a binding site of the nitrogen of the serine side chain is indicated. Noncovalent interactions were also confirmed by use of the analogue [*trans*-Pt(NH<sub>3</sub>)<sub>3</sub>]<sub>2</sub>μ-Pt(NH<sub>3</sub>)<sub>2</sub>{H<sub>2</sub>N(CH<sub>2</sub>)<sub>6</sub>NH<sub>2</sub>}(NO<sub>3</sub>)<sub>6</sub> (**III**, 0,0,0/*t,t,t*). The implications of these results for the mechanism of cellular uptake of polynuclear platinum complexes are discussed.

The membrane interactions of polynuclear platinum anticancer drugs were studied with liposomes as a biomembrane model using various calorimetric and spectroscopic techniques.

The three principal pharmacological factors affecting the cytotoxicity of platinum drugs are cellular uptake and efflux, the frequency and structure of target (DNA) adducts, and the extent of metabolizing reactions of sulfur-containing proteins and peptides. Much is known on the molecular mechanism of interactions with DNA (1–3) as well as the structures and products of reactions with sulfur nucleophiles such as methionine, cysteine, and glutathione (4–7). In contrast, less is known about the structural detail and

mechanism of cellular uptake, the first step in the cellular action of platinum drugs. Both passive and energy-dependent (activated) pathways exist for platinum complex uptake (8–10). The influence of the copper transport and efflux system on platinum status in cells has also been an area of considerable recent interest (11–13). Despite these advances in the understanding of platinum drug uptake and its role in cellular sensitivity and/or resistance, the interaction of platinum drugs with membranes has not been described in detail.

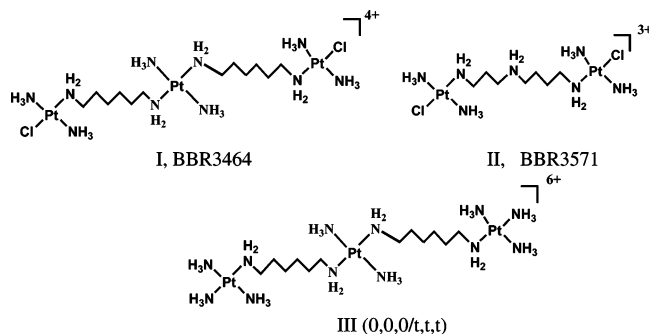
Di- and trinuclear platinum drugs contain two or three platinum centers linked by diamine chains (Scheme 1). The positively charged BBR3464 and BBR3571 exhibit significantly higher levels of cellular uptake than neutral cisplatin (14, 15) and a different pattern of DNA binding compared to those of cisplatin and other “classical” mononuclear platinum drugs (16–19). The electrostatic and hydrogen bonding interactions available to these molecules are important in their DNA interactions and also produce the most cytotoxic compounds (15). These “noncovalent” interactions

<sup>†</sup> This work was supported by NIH operating grants (RO1CA58754).

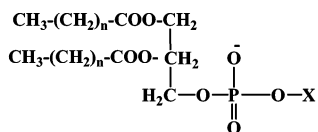
<sup>\*</sup> To whom correspondence should be addressed: Department of Chemistry, Virginia Commonwealth University, 1001 W. Main St., Richmond, VA 23220. Phone: (804) 828-6320. Fax: (804) 828-8599. E-mail: nfarrell@mail1.vcu.edu.

<sup>‡</sup> Department of Chemistry.

<sup>§</sup> Biochemistry Department.

Scheme 1: Structures of BBR3464 (I), BBR3571 (II), and a Noncovalent Analogue, III (0,0,0/*t,t,t*)

Scheme 2: Structure and Abbreviations of the Phospholipids Used in This Study



(X = H, PA; X=CH<sub>2</sub>CHNH<sub>2</sub>COOH, PS; X=CH<sub>2</sub>CH(OH)(CH<sub>2</sub>(OH), PG; X = (CH<sub>2</sub>)<sub>2</sub>NH<sub>3</sub><sup>+</sup>, PE; X=(CH<sub>2</sub>)<sub>2</sub>N(CH<sub>3</sub>)<sub>3</sub>, PC)

1,2-dipalmitoyl-*sn*-glycero-3-phosphatidic acid (DPPA) (n=14)

1,2-dipalmitoyl-*sn*-glycero-3-phosphatidyl-choline, (DPPC) (n=14)

1,2-dipalmitoyl-*sn*-glycero-3-phosphatidyl-ethanolamine (DPPE) (n=14)

1,2-dipalmitoyl-*sn*-glycero-3-phosphatidyl-serine (DPPS) (n=14)

1,2-dipalmitoyl-*sn*-glycero-3-phosphatidyl-glycerol (DPPG) (n=14)

1,2-Dihexanoyl-*sn*-Glycero-3-Phosphate (Monosodium Salt) (DHPA) (n=4)

1,2-Dihexanoyl-*sn*-Glycero-3-[Phosphatidyl-L-Serine] (Sodium Salt) (DHPS) (n = 4)

have been studied in the absence of formation of Pt–DNA bonds via analogous compounds capable of only noncovalent interaction such as **III** in Scheme 1 (20, 21). The noncovalent compounds strongly interact with DNA and induce unusual conformational effects, including cooperative binding of minor groove-binding ligands (20). Cellular uptake of these charged polynuclear molecules is remarkably enhanced in comparison to that of neutral cisplatin, even with compounds carrying a formal charge of +8 (22). These observations suggest that noncovalent (hydrogen bonding and electrostatic) interactions can be observed with other bimolecules involved in cellular uptake and metabolism. We have therefore begun a systematic study to examine the generality of these interactions and their relevance to the mechanism of action of polynuclear platinum drugs. In this paper, we examine the interactions of polynuclear platinum drugs with phospholipids as model systems for biomembranes and their possible relevance to cellular uptake.

Liposomes are a good model for biomembranes and have been widely used for studying drug delivery and drug interaction with the phospholipid bilayer (23–26). Less has been reported about the interactions of platinum anticancer drugs with lipids (27–29). This paper describes a study of the interactions between di- and trinuclear platinum drugs and five different phospholipids chosen for the diversity of charge and headgroup [DPPS, DPPA, DPPE, DPPG, and DPPC (see Scheme 2)] using differential scanning calorimetry (DSC), inductively coupled plasma (ICP), <sup>31</sup>P nuclear magnetic resonance spectroscopy (NMR), and electrospray

ionization mass spectrometry (ESI-MS) methods. The results indicate that the interactions of phospholipids with BBR3464 and BBR3571 are dependent on charge and occur in a two-step mechanism in which the noncovalent interaction is the first stage.

## MATERIALS AND METHODS

**Materials.** BBR3464 and BBR3571 were prepared according to the literature procedures (30, 31). DPPS, DPPA, DPPC, DPPG, and DPPE were purchased from Avanti Inc. Pipes buffer solution was prepared by mixing 10 mM pipes, 100 mM NaCl (or 100 mM NaClO<sub>4</sub>), and 1 mM EGTA, with the pH adjusted to 7.40 with 1 M NaOH.

**Liposome Preparation [Large Unilamellar Vesicles (LUV)].** Phospholipid (3.5 mmol) was dissolved in a minimum amount of chloroform. A dry thin film was obtained by slow evaporation of this lipid chloroform solution. The film was dried overnight under vacuum and then hydrated in 2.5 mL pipes buffer (either in the absence or in the presence of platinum compounds). When the liposome was prepared in the buffer in the presence of the platinum complex, the initial molar ratio of lipids to platinum compound was 9:1. After 10 freeze–thaw cycles, the suspension was extracted with a Mini-Extruder (Avanti Inc.) through 400 nm polycarbonate filter membranes.

**Differential Scanning Calorimetry (DSC).** DSC was performed using a Nano II differential scanning calorimeter, N-DSC II, model 6100 (Calorimetry Sciences Corp., American Fork, UT). Before analysis, samples were degassed under vacuum for 10–15 min. For each analysis, a buffer–buffer scan was performed to establish a baseline. Subsequently, the reference buffer and liposome samples (0.33 mL each) were loaded in their appropriate cells and scanned from 25 to 75 °C at a heating rate of 1 °C/min. Enthalpy, entropy, and melting temperatures were calculated using CpConvert version 2.2.1 (applied Thermodynamics, LLC).

**Binding Assay.** The binding of platinum drugs with model membranes was studied as follows. DPPA, DPPS, DPPG, DPPE, and DPPC liposomes (100 μL) were mixed with 900 μL of BBR3571 or BBR3464 (~0.01–0.15 mM). The suspensions were incubated for 5 days in the dark at 37 °C and then centrifuged for 80 min at 17000g and 25 °C. The top 500 μL solutions were collected for the determination of the amount of free platinum by ICP-OES.

In the kinetic studies, a 1 mL DPPA/DPPS solution (3.2 mM) was mixed with 9 mL of BBR3464/BBR3571 (0.11 mM) and incubated at 37 °C in the dark. One milliliter of the suspension was taken and centrifuged. The platinum concentration of the solution was measured by ICP-OES using the same method at different times (the first one was taken after mixing for 20 min and then every 24 h for 7 days).

**Platinum Determination.** The liposome/platinum solutions were digested by EPA method 3050B and diluted to 10 mL. The concentration of Pt was determined by using VISTA-MPX CCD simultaneous ICP-OES. The following conditions were used: power of 1.00 kW, plasma flow of 15.0 L/min, auxiliary flow of 1.50 L/min, nebulizer pressure of 1 kPa, and replicated read time of 5 s. Five standard samples of 0.5000, 1.000, 5.000, 10.0000, and 15.000 μM K<sub>2</sub>PtCl<sub>4</sub> and a blank solution were used. Three wavelengths of 214.424,

265.945, and 306.471 nm were chosen to monitor the Pt concentration.

**Phosphorus Determination.** Phosphorus concentrations for all the liposomes used in the binding and kinetic studies were measured by VISTA-MPX CCD simultaneous ICP-OES to calculate the binding ratio between platinum drugs and lipids. Before the measurement, a 500  $\mu$ L liposome suspension was digested by EPA method 3050B and diluted to 10 mL. The polyboost was turned on 30 min before the measurement. The same conditions that were used for platinum measurement were used except the power was increased to 1.2 kW. Three standard samples of 0.500, 1.000, and 5.000 ppm ( $\text{NH}_4\text{H}_2\text{PO}_4$ ) were used as standard samples. Wavelengths of 177.434, 178.222, and 213.618 nm were chosen to monitor the phosphorus concentration.

**NMR Spectroscopy.** One-dimensional  $^{31}\text{P}$  NMR spectra were recorded on a Varian Mercury series 300 MHz NMR spectrometer using an AutoSwitchable four-nucleus 5 mm probe.  $^{31}\text{P}$  spectra were referenced to trimethyl phosphate (TMP) at 0 ppm. The resonance frequency for  $^{31}\text{P}$  nuclei was set at 121.387 MHz. BBR3464 and BBR3571 solutions were incubated with DPPS and DPPA liposomes at a 1:2 molar ratio. After 5 days, the liposomes were extracted via the published method (32) and dried under vacuum. The NMR samples were prepared in 0.5 mL of  $\text{CDCl}_3$ .

**Electrospray Ionization Mass Spectrometry (ESI-MS) Method.** BBR3464 and BBR3571 were mixed with DPPA and DPPS liposomes [prepared in chloride or chloride-free pipes buffer (pH 7.4)] at a molar ratio of 1:2.5. After incubation for 5 days at 37  $^{\circ}\text{C}$ , the suspensions were extracted with chloroform. The extract was lyophilized and then dissolved in a  $\text{MeOH}/\text{CHCl}_3$  mixture (1:1) for ESI-MS measurement. Electrospray ionization mass spectra were recorded with a Finnigan LCQ ion-trap electrospray meter (LCQ-MS) in positive ion mode. The employed voltage at the electrospray needles was 4.5 kV, and  $\text{N}_2$  sheath gas and Aux/sweep gas were used. The capillary was heated to 150  $^{\circ}\text{C}$ . The solutions were injected into the ESI source directly at a flow rate of 3.0  $\mu\text{L}/\text{min}$ . Tandem mass and zoom scan were used to analyze the structure of the product in the experiments. Helium gas was admitted directly into the ion trapping efficiency and as the collision gas in the collision-induced dissociation (CID) experiment. A maximum ion injection time of 500 ms along with 10 scans was set. To induce collision activation, the relative collision energy was controlled to 10–30% of maximum, depending on the precursor ions and  $\text{MS}^n$ . In  $\text{MS}/\text{MS}$  and  $\text{MS}^n$  experiments, an isolation width of 6–12 for the precursor ions was used to allow the Pt isotopic signature to be observed.

## RESULTS

### Interaction of Phospholipids with Polynuclear Platinum Drugs Studied by Differential Scanning Calorimetry (DSC)

**DPPA with BBR3464 and BBR3571.** Differential scanning calorimetry is useful in obtaining transition temperatures and thermodynamic parameters for the interaction between drugs and membranes. Figure 1A shows the DSC results of liposome DPPA in the absence and presence of the platinum compounds. The major transition temperature of DPPA was

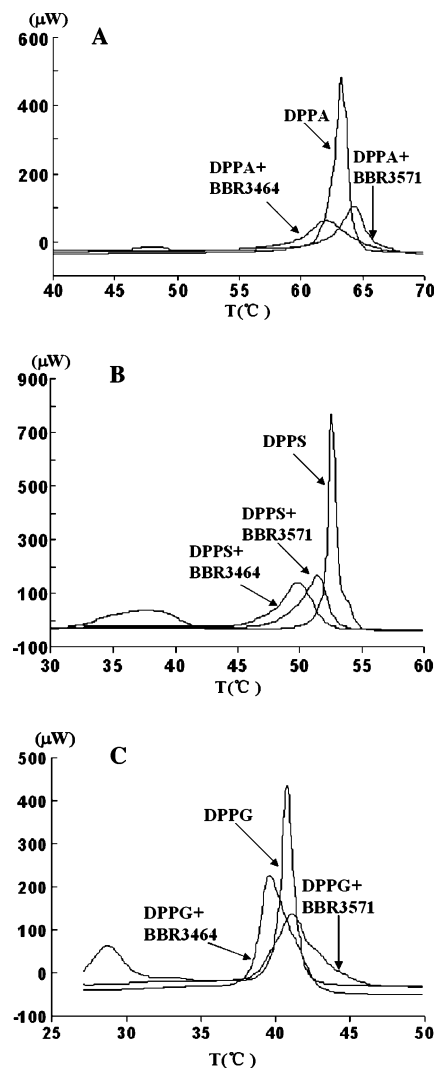


FIGURE 1: DSC results for (A) DPPA, (B) DPPS, and (C) DPPG in the presence and absence of BBR3464 and BBR3571 in pipes buffer (pH 7.4).

64.0  $^{\circ}\text{C}$ , and a pretransition peak at 47  $^{\circ}\text{C}$  was observed. The transition temperature decreased to 62  $^{\circ}\text{C}$  in the presence of BBR3464 and increased to 65.7  $^{\circ}\text{C}$  in the presence of BBR3571. In both cases, the pretransition peak disappeared. The  $\Delta H$  and  $\Delta S$  values of free phospholipid were 7.5 kcal/mol and 0.023 kcal  $\text{mol}^{-1}$   $\text{K}^{-1}$ , respectively. In the presence of BBR3464 or BBR3571, the  $\Delta H$  decreased to 5.5 or 5.9 kcal/mol, respectively, and  $\Delta S$  decreased to 0.018 kcal  $\text{mol}^{-1}$   $\text{K}^{-1}$  in both cases (Table 1).

**DPPS with BBR3464 and BBR3571.** The major transition temperature of DPPS liposome was 52.5  $^{\circ}\text{C}$ , and the pretransition temperature was 38.0  $^{\circ}\text{C}$ , consistent with the published data (33). The enthalpy ( $\Delta H$ ) and entropy ( $\Delta S$ ) were 11.0 kcal/mol and 0.030 kcal  $\text{mol}^{-1}$   $\text{K}^{-1}$ , respectively. In presence of BBR3464 and BBR3571, the pretransition peak again disappeared and the decrease in the transition temperature was larger with BBR3464 ( $T_m = 49.8$   $^{\circ}\text{C}$ ) than with BBR3571 ( $T_m = 51.4$   $^{\circ}\text{C}$ ) (Figure 1B). The enthalpy  $\Delta H$  and entropy  $\Delta S$  also decreased (Table 1).

**DPPG with BBR3464 and BBR3571.** The DSC results of DPPG liposomes with BBR3464 and BBR3571 are shown in Figure 1C. The transition temperature of DPPG liposomes was 40.7  $^{\circ}\text{C}$ , and the  $\Delta H$  and  $\Delta S$  values were 8.3 kcal/mol

Table 1: DSC and Thermodynamic Parameters for Different Liposomes in the Presence and Absence of Platinum Drugs BBR3464 and BBR3571 in Pipes Buffer (pH 7.4)

	$T_m$ (°C)	$\Delta H$ (kcal/mol)	$\Delta S$ (kcal mol <sup>-1</sup> K <sup>-1</sup> )
DPPA	64.0	7.5	0.023
DPPA and BBR3464	62.0	5.5	0.018
DPPA and BBR3571	65.7	5.9	0.018
DPPS	52.5	8.7	0.030
DPPS and BBR3464	49.8	6.4	0.021
DPPS and BBR3571	51.4	6.6	0.020
DPPG	40.7	8.3	0.028
DPPG and BBR3464	39.2	6.7	0.021
DPPG and BBR3571	40.5	6.6	0.021
DPPC	41.7	6.5	0.020
PPC and BBR3464	41.7	6.5	0.021
DPPC and BBR3571	41.7	6.5	0.021
DPPE	64.1	8.1	0.024
DPPE and BBR3464	64.1	8.1	0.024
DPPE and BBR3571	64.1	8.1	0.024

and 0.028 kcal mol<sup>-1</sup> K<sup>-1</sup>, respectively. In the presence of BBR3464, the transition temperature decreased to 39.2 °C. A very slight change was observed in the presence of BBR3571. The  $\Delta H$  decreased to 6.7 and 6.6 kcal/mol in the presence of BBR3464 and BBR3571, respectively.  $\Delta S$  values were identical and decreased to 0.021 kcal mol<sup>-1</sup> K<sup>-1</sup> for both compounds (Table 1).

**DPPE and DPPC.** The transition temperatures of DPPC and DPPE were 41.7 and 64.1 °C, respectively (Figures S1 and S2 of the Supporting Information). There was very little or no change in the transition temperature or the thermodynamic values of the liposomes upon incubation with BBR3464 or BBR3571 (see Table 1). The pretransition in DPPC was

observed at 35.0 °C and was unaffected by the presence of the platinum drugs, which indicated there was almost no interaction between the zwitterionic phospholipids and the polynuclear platinum drugs.

#### Interaction of Phospholipids with Polynuclear Platinum Drugs Studied by Inductively Coupled Plasma Spectrometry (ICP)

To examine the extent of drug–phospholipid interaction, ICP was used to quantify the platinum binding. Simultaneously, the phosphorus concentration of the liposome was determined to calculate a binding ratio  $r_b$  (moles of Pt complex per mole of P<sub>i</sub>). Figure 2 shows the binding profiles between phospholipid and BBR3464 in (a) a chloride-free solution and (b) a 100 mM NaCl solution. Significant binding was observed for the three negatively charged phospholipids DPPA, DPPS, and DPPG. The binding ratio of DPPG is lower than that of DPPS and DPPA. The binding ratios ( $r_b$ ) of BBR3464 (0.14 mM) to DPPG, DPPA, and DPPS are 0.210, 0.285, and 0.315 in chloride-free solution, respectively, which changed to 0.17, 0.225, and 0.236, respectively, in 100 mM NaCl buffer. Thus, the binding ratios of BBR3464 to the phospholipids decrease slightly but not significantly in the presence of 100 mM NaCl. The  $r_b$  values of the platinum complexes with the zwitterionic phospholipids DPPE and DPPC were low in both the presence and the absence of chloride. The binding ratios of BBR3464 to DPPA are slightly higher than the ratios of BBR3464 to DPPS at the highest concentration used in both solutions. Figure 3 shows the binding of BBR3571 to the different phospholipids. The results are very similar to those of BBR3464, and

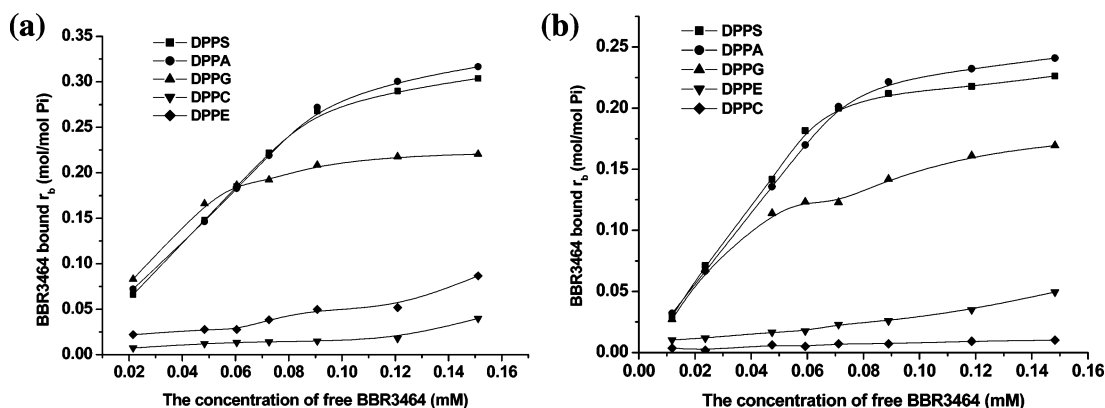


FIGURE 2: Binding of BBR3464 to different phospholipids in (a) chloride-free and (b) 100 mM NaCl pipes buffer (pH 7.4) after incubation for 5 days at 310 K.

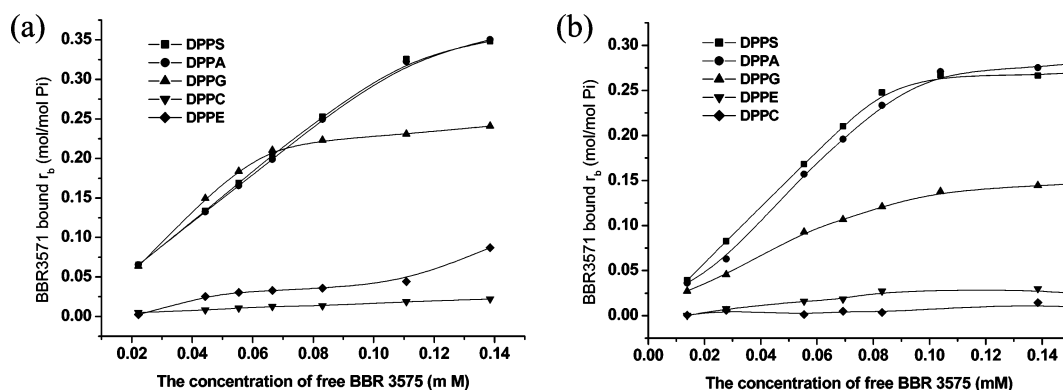


FIGURE 3: Binding of BBR3571 to different phospholipids in (a) chloride-free and (b) 100 mM NaCl pipes buffer (pH 7.4) after incubation for 5 days at 310 K.



Table 2:  $^{31}\text{P}$  NMR Results for Free Lipids and Lipids after Incubation with BBR3464 and BBR3571 in Different Buffers

lipid	$^{31}\text{P}$ $\delta$ (ppm)	
	$\text{Cl}^-$ -free buffer	100 mM $\text{Cl}^-$ buffer
free DPPA	−0.41	
DPPA and BBR3464	6.56, −1.44	6.54, −1.60
DPPA and BBR3571	6.46, −1.28	6.47, −1.25
free DPPS	−2.08	
DPPS and BBR3464	−2.46, −2.47	−2.49, −2.51
DPPS and BBR3571	−2.48, −2.52	−2.33, −2.44
free DPPG	−1.43	
DPPG and BBR3464	3.62, −2.36	−2.32
DPPG and BBR3571	−2.25	−2.00
DPPA and AH44	−1.51	
DPPS and AH44	2.69	

the lack of reactivity to DPPE and DPPC was also observed. The binding ratios ( $r_b$ ) of BBR3571 (0.14 mM) to DPPG, DPPA, and DPPS were 0.23, 0.295, and 0.35, respectively, in the absence of chloride solution. The  $r_b$  values decreased to 0.140, 0.260, and 0.275, respectively, in 100 mM NaCl.

**Kinetic Study.** The kinetics of binding of polynuclear platinum drug to DPPA and DPPS in chloride-free pipes buffer was also studied by ICP-OES. The concentrations of BBR3464 and BBR3571 were 0.11 mM in this study. The results showed that an initial rapid binding occurred within the first 20 min followed by a further slow interaction toward equilibrium (Figures S3 and S4 of the Supporting Information). After 24 h, only modest increases in the binding ratio were observed. The binding ratios in all cases were in agreement with those obtained above. It is reasonable to interpret the initial reaction as noncovalent, dominated presumably by electrostatic and hydrogen bonding interactions followed by slower formation of the platinum–phospholipid complex. All samples for DSC and spectroscopy were measured after being incubated for 5 days to maximize the amount of covalently bound species formed in the heterogeneous reaction solution used.

#### Structural Characterization of the Interaction of Phospholipids with Polynuclear Platinum Drugs by $^{31}\text{P}$ NMR Spectroscopy

To examine the structural nature of the drug–phospholipid interaction, NMR spectroscopy and mass spectrometry were used. After incubation of the liposomes with BBR3464 and BBR3571 at 37 °C in the presence or absence of chloride buffer (pH 7.4), the phospholipids were extracted with chloroform and  $^{31}\text{P}$  NMR spectra were recorded. The results are summarized in Table 2. The  $^{31}\text{P}$  NMR spectrum of the incubation product of BBR3464 with DPPA showed two peaks at 6.56 and −1.44 ppm, compared to the chemical shift of free DPPA at −0.41 ppm. Because of the possibility of preferential extraction of either species giving rise to these signals, no attempts were made to integrate them and no estimates of relative proportions of the species present are made. The relatively large downfield shift of the signal at 6.56 ppm is perfectly consistent with the formation of a platinum–phosphato species (34, 35). Similar chemical shifts were observed for BBR3571 (6.46 and −1.28 ppm). The observation of upfield shifts suggests the possibility of a noncovalent (electrostatic and/or hydrogen bonding) interaction between the DPPA and BBR3464 or BBR3571. To

examine this point, the +6 noncovalent analogue **III** (0,0,0/ $t,t,t$ ), where the chloride leaving groups are replaced by the inert ammonia ligands to prevent covalent bond formation (Scheme 1) (20, 21), was incubated with DPPA in 100 mM NaCl pipes buffer. The  $^{31}\text{P}$  NMR spectrum exhibited only one upfield signal at −1.51 ppm ( $\Delta\delta = 1.10$  ppm), completely consistent with our interpretation of noncovalent interactions.

The interaction with DPPG followed a pattern similar to that of DPPA. In the presence of BBR3464,  $^{31}\text{P}$  signals appear at 3.62 and −2.36 ppm compared to the chemical shift of free DPPG at −1.43 ppm. The upfield shift again indicates a noncovalent interaction. The downfield signal of the  $^{31}\text{P}$  spectrum at 3.62 ppm was of weak intensity but consistent with covalent bond formation between BBR3464 and the headgroup of DPPG. In 100 mM chloride buffer, only the upfield signal at −2.33 ppm was observed. In the case of BBR3571, evidence for only the noncovalent interaction (at −2.24 ppm in absence of chloride buffer and −2.00 ppm in the presence of chloride buffer) was obtained and no downfield signals were observed. It is possible that these observations are due to preferential extraction and/or the fact that DPPG is a phosphodiester and the phosphate oxygen has weaker coordinating ability than DPPA.

In both DPPA and DPPG, the downfield shift is clear evidence of formation of a platinum–phosphate bond. In contrast, only slight upfield chemical shifts of peaks to −2.46 and −2.47 ppm were observed after the incubation of DPPS with BBR3464 compared to the free DPPS at −2.08 ppm. The presence of two distinct peaks is clearly discernible, despite the high degree of similarity in the chemical shift (Figure S5). The presence of two peaks is also seen for BBR3571 incubation, and the chemical shift values vary little in the absence or presence of chloride (Table 2). Incubation of DPPS with the noncovalent **III** (0,0,0/ $t,t,t$ ) gave one  $^{31}\text{P}$  signal at −2.70 ppm indicating that one of the two peaks observed for BBR3464 and BBR3571 arises from the noncovalent interaction. The absence of a downfield signal would imply therefore that the phosphate group is not the origin of the covalent binding site of DPPS. In separate experiments,  $\{^1\text{H},^{15}\text{N}\}$  HSQC NMR spectra of  $[^{15}\text{N}]\text{B}-\text{BR3464}$  incubated with DHPS (see Scheme 2) exhibited chemical shifts indicative of Pt–N binding, consistent with an expected preference for the nitrogen, rather than carboxylate oxygen, of the serine group (data not shown).

#### Structural Characterization of the Interaction of Phospholipids with Polynuclear Platinum Drugs by ESI-Mass Spectrometry

To further examine the nature of the covalent interaction between phospholipids and polynuclear platinum compounds, samples for mass spectrometry were extracted from the suspension of BBR3464 with DPPA and DPPS and introduced into the electrospray ionization mass spectrometer in a 1:1 MeOH/ $\text{CHCl}_3$  mixture. For DPPA, a major peak at  $m/z$  1106.5 and a minor peak at  $m/z$  738.2 were observed (Figure 4). The peak at  $m/z$  1106.5 was split to 0.5 unit and the peak at  $m/z$  738.2 to 0.33 unit, which suggested that they are +2 and +3 ions for the same species, respectively. This species was assigned to the ion of  $[\text{Pt}_3(\text{NH}_3)_6\{\text{NH}_2(\text{CH}_2)_6\text{NH}_2\}_2(\text{DPPA})_2]^{2+}$  (**1**), in which the two chlorides of BBR3464

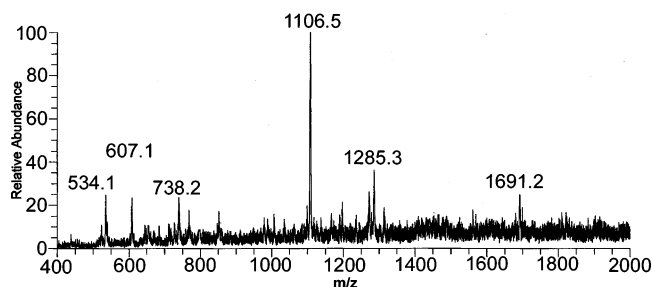


FIGURE 4: ESI-MS spectrum of the sample extracted from the suspension of DPPA with BBR3464.

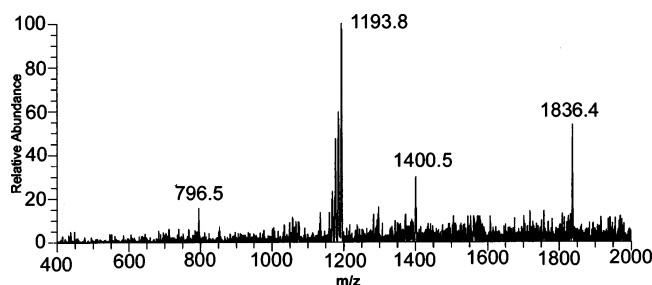


FIGURE 5: ESI-MS spectrum of the sample extracted from the suspension of BBR3464 with DPPS.

were replaced with two DPPA<sup>-</sup> ligands. Along with these two peaks, a peak at  $m/z$  534.1 corresponding to the +3 ion of  $[\text{Pt}_3(\text{NH}_3)_6\{\text{NH}_2(\text{CH}_2)_6\text{NH}_2\}_2(\text{DPPA})\text{Cl}]^{3+}$ , in which only one of the chloride ligands is displaced, was also observed. The isotopic distribution of the peak was consistent with calculated results (Figure S6). The principal fragment ions observed in MS/MS and MS<sup>n</sup> modes from CID experiments conducted on the peak at  $m/z$  1106.5 are shown in Table S1. The fragment ions at  $m/z$  1098.1 and 1089.5 were observed in the MS/MS spectrum, corresponding to loss of 17 and 34 amu from the precursor, corresponding to one and two ammonia ligands, respectively. The six ammonia ligands were lost sequentially until MS<sup>4</sup> was carried out when the loss of a DPPA fragment was also observed, indicating that the platinum–phosphate bond is very stable under these conditions.

For the extracted sample from the suspension of BBR3464 with DPPS, a principal peak was observed at  $m/z$  1193.8, assigned to the +2 charged ion of  $[\text{Pt}_3(\text{NH}_3)_6\{\text{NH}_2(\text{CH}_2)_6(\text{NH}_2)\}_2(\text{DPPS})_2]^{2+}$  (**2**) (Figure 5). The next most prominent peak observed is that at  $m/z$  1836.4. The splitting of the isotopic peaks to 0.33 unit indicates a +3 charged species, identified as a species containing two  $[\text{Pt}_3(\text{NH}_3)_6\{\text{NH}_2(\text{CH}_2)_6(\text{NH}_2)\}_2(\text{DPPS})_2]^{2+}$  units and one DPPS. An analogous peak that was less intense at  $m/z$  1691.2 was observed in the reaction of BBR3464 with DPPA (Figure 4). This peak can also be assigned to the +3 charged species comprised of two  $[\text{Pt}_3(\text{NH}_3)_6\{\text{NH}_2(\text{CH}_2)_6(\text{NH}_2)\}_2(\text{DPPA})_2]^{2+}$  units and one additional DPPA<sup>-</sup> unit. The hydrophobic interaction of fatty acid chains between these ions and the less polar solvent used for mass spectrometry could be the reason for the formation and observation of these novel species.

When the peak at  $m/z$  1193.8 was chosen as a precursor for MS/MS, sequential loss of four NH<sub>3</sub> ligands occurred (see Table S2). In contrast to the DPPA example, however, no subsequent loss of phospholipid was observed. Instead, further MS/MS selection results in breakdown of the phospholipid structure, possibly reflecting the difference in the

mode of binding of the Pt to DPPA and DPPS (see Figure S7). Notable is the peak at  $m/z$  835.2 even though it is of low intensity. This peak also shows a +2 ion and can be assigned to a 96 amu fragment lost from species at  $m/z$  883.5, attributed to a HPO<sub>4</sub> fragment. The observation of this fragment suggests that the atom covalently bound to Pt in DPPS could be in the serine headgroup, rather than phosphate, in  $[\text{Pt}_3(\text{NH}_3)_6\{\text{NH}_2(\text{CH}_2)_6(\text{NH}_2)\}_2(\text{DPPS})_2]^{2+}$ , consistent with the <sup>31</sup>P NMR results.

The ESI-MS results of the samples from the reactions of BBR3571 with DPPA and DPPS are very similar to those of the samples from BBR3464. A peak at  $m/z$  949.9 corresponding to  $[\text{Pt}_2(\text{NH}_3)_4\{(\text{NH}_2)(\text{CH}_2)_3\text{NH}(\text{CH}_2)_4\text{NH}_2\}-(\text{DPPA})_2]^{2+}$  (**3**) was observed for the sample extracted from the suspension of BBR3571 with DPPA (see Figure S8). A peak at  $m/z$  644.2 corresponding to one DPPA covalently bound to BBR3571,  $[\text{Pt}_2\{(\text{NH}_2)(\text{CH}_2)_3\text{NH}(\text{CH}_2)_4\text{NH}_2(\text{NH}_3)_4\}-(\text{DPPA})\text{Cl}]^{2+}$ , was also observed. A peak at  $m/z$  1898.1 assigned as the +2 ion of  $[\text{Pt}_2(\text{NH}_3)_4\{(\text{NH}_2)(\text{CH}_2)_3\text{NH}(\text{CH}_2)_4\text{NH}_2\}(\text{DPPA})_2]^{2+}$  was also observed in this spectrum. No evidence of further associated DPPA, as in the case of BBR3464, was observed in this species, probably because of the smaller overall positive charge of BBR3571 versus BBR3464. For the sample of BBR3571 with DPPS, a peak at  $m/z$  1037.5 corresponding to  $[\text{Pt}_2\{(\text{NH}_2)(\text{CH}_2)_3\text{NH}(\text{CH}_2)_4\text{NH}_2(\text{NH}_3)_4\}(\text{DPPS})_2]^{2+}$  was observed. The same species were observed in all the samples extracted from a 100 mM NaCl buffer suspension.

## DISCUSSION AND CONCLUSIONS

The combined results unequivocally confirm both noncovalent and covalent contributions to the interactions of phospholipids with positively charged polynuclear platinum complexes. The pattern of binding affinity (DPPA > DPPS > DPPG ≫ DPPE > DPPC) is easily understood by considering the amphiphilic cationic nature of the complexes and the overall charge of the amphiphilic phospholipids. The higher binding ratio with DPPA in comparison to those with DPPS and DPPG may be due to the smaller phosphate group and higher electronic density of DPPA when compared to DPPS and DPPG. The ratios of binding of both BBR3464 and BBR3571 to the phospholipids are significantly greater than that of cisplatin (see Table 3), both in the absence and in the presence of chloride. Interestingly, both <sup>31</sup>P NMR spectroscopy and ESI-mass spectrometry indicated covalent interactions of DPPA and DPPS even in 100 mM NaCl. <sup>1</sup>H, <sup>15</sup>N HSQC NMR studies on the kinetics and equilibrium of aquation of BBR3464 indicated that the equilibrium lies to the left (with a high  $k_{-1}$ ), and under physiological conditions, more than 97% of the compound is in the chloride form (36). Two interesting points are, therefore, that bond formation of weakly coordinating phosphate (DPPA) takes place at all and that the binding of BBR3464 and BBR3571 is significantly stronger than that of *cis*-DDP under all conditions and for all phospholipids (see Table 3). The strong noncovalent interaction observed by <sup>31</sup>P NMR spectroscopy and the kinetic ICP experiments suggests that this “preassociation” mechanism could facilitate chloride displacement and also effectively reduce the chloride concentration in the vicinity of the binding site. Analogous observations have been made in examining the rate of aquation of BBR3464 in the presence of DNA (37). A preassociation would be

Table 3: Binding of Platinum to Different Phospholipids at a Fixed Free Platinum Compound Concentration of 0.10 mM (moles of platinum compound per mole of P<sub>i</sub>)

phospholipid	BBR3464		BBR3571		<i>cis</i> -DDP(29)	
	Cl <sup>-</sup> -free	100 mM Cl <sup>-</sup>	Cl <sup>-</sup> -free	100 mM Cl <sup>-</sup>	Cl <sup>-</sup> -free	100 mM Cl <sup>-</sup>
DPPA	0.275	0.225	0.300	0.260	0.0185	0.0056
DPPS	0.265	213	0.295	0.260	0.0225	<0.001
DPPG	0.210	1.45	0.225	0.125	0.0015	<0.001
DPPE	0.050	0.025	0.040	0.025	<0.001	<0.001
DPPC	0.010	0.008	0.011	0.007	<0.001	<0.001

expected to be stronger with a higher positive charge and would correlate with the observed binding ratios (BBR3464 > BBR3571 > cisplatin carrying +4, +3, and 0 charges, respectively). The mass spectrometric observation of an unusual association of an additional DPPA molecule with the coordinated species may reflect further aggregation of the amphiphilic anion.

The molecular details of the preassociation and how the nature of this interaction changes the physical state of the membrane cannot be readily discerned from these experiments. Some idea of the exact nature of the interaction can, however, be obtained from the thermodynamic studies of the transition temperature. Phospholipids exhibit thermotropic and lyotropic phase behavior. Hydrated biomolecular lamellar phases are formed when the phospholipid film is dispersed in excess water, in which the lipid molecules are packed in a quasi-crystalline two-dimensional lattice (gel phase  $L_{\beta}$ ) or remain in a lamellar arrangement but show higher two-dimensional fluidity in a liquid crystalline phase ( $L_{\alpha}$ ) (24). Transition between these phases can be induced by temperature changes. The transition temperature, enthalpy, or entropy of the gel to the liquid phase transition is altered by drug interaction, and quantification of these parameters provides information about the nature of the interaction. Usually, an increase in the transition temperature is caused by of the negatively charged phospholipids by positively charged ions such as Ca<sup>2+</sup> or Mg<sup>2+</sup> and indicates reduced fluidity of the membrane (38). Any drug entering the bilayer will modify the interacting forces between the lipid alkyl chains and affect the thermogram. Peak broadening with a decrease or increase in the transition temperature suggests the location of the drug in the cooperative region of the first eight carbons of the alkyl chain (C2–C8). A decrease in the transition temperature without broadening implies the interaction is in the C12–C16 region (24). The total enthalpy change associated with the main lipid chain melting is related to molecular packing of alkyl chains (26, 39). In the case of the polynuclear platinum complexes, the decrease or increase (DPPA in the presence of BBR3571) in the transition temperature and broadening of the peaks for DPPS, DPPA, and DPPG liposomes upon incubation with BBR3464 or BBR3571 suggested that the platinum drugs affected the C2–C8 region of the alkyl chain due to the hydrophilic property of these compounds. The perturbation of phospholipid bilayer packing resulted in decreases in entropy and enthalpy. These observations suggested that overall charged platinum compounds BBR3464 and BBR3571 interact strongly with negatively charged liposomes not only at the phosphate headgroup but also at the core of bilayer.

The negatively charged lipids PS and PA are involved in many membrane functions such as signal transduction (40, 41), protein kinase C activity regulation (42), oxidative

phosphorylation, and cell proliferation (43, 44). How platinum–drug interactions affect signaling remains to be determined. Cisplatin–DPPS interactions are not considered to play a direct role in cytotoxicity (27). In contrast, studies on the cisplatin-sensitive A549 and cisplatin-resistant A549/DDP cells clearly indicated that components and properties of membrane phospholipids of the two cell lines were significantly different during the apoptotic process when they were treated with a clinically relevant dose of cisplatin (45). The plasma membrane plays an important role in the control of intracellular concentration and the efflux and influx of drugs. Many anticancer drugs show membrane effects via weak hydrophobic interaction or via electrostatic binding to membrane phospholipids before entering the cytoplasm, as indicated here. A hitherto unappreciated point demonstrated here is that the nature of the formation of the bond with phosphate oxygen versus that with serine nitrogen may also affect the dynamic properties of the drug–phospholipid conjugate. The uptake mechanism of platinum anticancer drugs is still unclear. Within the polynuclear platinum series, higher charge is actually associated with faster uptake even up to a formal charge of +8 (22). The strong electrostatic interaction between negatively charged lipids DPPS, DPPS, and DPPG and positively charged BBR3464 and BBR3571 may suggest a model for the uptake of the polynuclear platinum drugs. An attractive hypothesis is that a phosphate “shuttle” involving the formation and breaking of the relatively labile phosphate bond could assist in the transport of drugs across membranes. The growing recognition of the importance of cellular uptake and efflux mechanisms in determining clinical resistance to platinum drugs suggests that the details of the phospholipid interaction are worthy of more detailed examination in delineating the role and consequences of platinum–membrane binding in platinum-sensitive and -resistant cells. Finally, chemical and structural differences found in interactions of the polynuclear platinum and cisplatin with different liposomes should be considered when attempting to enhance the efficiency of drug treatment through targeted delivery systems and in designing new anticancer drugs.

## ACKNOWLEDGMENT

We thank Drs. S. Berners-Price and J. Zhang and J. Moniodis for stimulating discussions and John B. Mangrum for helping to determine the experimental condition for lipid ESI-MS measurement.

## SUPPORTING INFORMATION AVAILABLE

ESMS spectra of BBR3571 with DPPA, tandem mass analysis results and spectra of the products of the reactions between BBR3464 and DPPA/DPPS, DSC results of DPPE



and DPPC liposomes, kinetics of binding of BBR3464 and BBR3571 to DPPA/DPPS membranes, and  $^{31}\text{P}$  NMR spectra of BBR3464 and BBR3571 with DPPS. This material is available free of charge via the Internet at <http://pubs.acs.org>.

## REFERENCES

1. Kelland, L. R., and Farrell, N., Eds. (2000) Platinum-Based Drugs in Cancer Therapy, in *Cancer Drug Discovery and Development* (Teicher, B. A., Ed.) Humana Press, Totowa, NJ.
2. Lippert, B., Ed. (1999) in *Cisplatin: Chemistry and biochemistry of a leading anticancer drug*, Wiley-VCH, Weinheim, Germany.
3. Jamieson, E. R., and Lippard, S. J. (1999) Structure, recognition, and processing of cisplatin-DNA adducts, *Chem. Rev.* 99, 2451–2466.
4. Reedijk, J. (1999) Why does cisplatin reach guanine-N7 with competing S-donor ligands available in the cell? *Chem. Rev.* 99, 2499–2510.
5. Peleg-Shulman, T., and Gibson, D. (2001) Cisplatin-protein adducts are efficiently removed by glutathione but not by 5'-guanosine monophosphate, *J. Am. Chem. Soc.* 123, 3171–3172.
6. Teuben, J. M., Zubiri, M. R. I., and Reedijk, J. (2000) Glutathione readily replaces the thioether on platinum in the reaction with  $[\text{Pt}(\text{dien})(\text{GSMe})]^{2+}$  (GSMe = S-methylated glutathione): A model study for cisplatin-protein interactions, *Dalton Trans.* 3, 369–372.
7. Murdoch, P. D. S., Kratochwil, N. A., Parkinson, J. A., Partriarca, M., and Sardler, P. J. (1999) A novel dinuclear diamminoplatinum(II) glutathione macrochelate, *Angew. Chem., Int. Ed.* 38, 2949–2951.
8. Kartalou, M., and Essigmann, J. M. (2001) Mechanisms of resistance to cisplatin, *Mutat. Res.* 478, 23–43.
9. Wang, D., and Lippard, S. J. (2005) Cellular processing of platinum anticancer drugs, *Nat. Rev. Drug Discovery* 4, 307–320.
10. Marverti, G., and Andrew, P. A. (1996) Stimulation of cis-diamminedichloroplatinum(II) accumulation by modulation of passive permeability with genistein: An altered response in accumulation-defective resistant cells, *Clin. Cancer Res.* 2, 991–999.
11. Ishida, S., Lee, J., Thiele, D. J., and Herskowitz, I. (2002) Uptake of the anticancer drug cisplatin mediated by the copper transporter Ctr1 in yeast and mammals, *Proc. Natl. Acad. Sci. U.S.A.* 99, 14298–14302.
12. Safaei, R., Holzer, A. K., Katano, K., Samimi, G., and Howell, S. B. (2004) The role of copper transporters in the development of resistance to Pt drugs, *J. Inorg. Biochem.* 98, 1607–1613.
13. Samimi, G., and Howell, S. B. (2005) Modulation of the cellular pharmacology of JM118, the major metabolite of satraplatin, by copper influx and efflux transporters, *Cancer Chemother. Pharmacol.* 17, 1–8.
14. Roberts, J. D., Peroutka, J., Beggiolin, G., Manzotti, C., Piazzoni, L., and Farrell, N. (1999) Comparison of cytotoxicity and cellular accumulation of polynuclear platinum complexes in L1210 murine leukemia cell lines, *J. Inorg. Biochem.* 77, 47–50.
15. Farrell, N. (2000) Polynuclear charged platinum compounds as a new class of anticancer agents. Toward a new paradigm, in *Platinum-Based Drugs in Cancer Therapy* (Kelland, L. R., and Farrell, N., Eds.) pp 321–338, Humana Press, Totowa, NJ.
16. McGregor, T. D., Kasparkova, J., Nepelchova, K., Novakova, O., Penazova, H., Vrana, O., Brabec, V., and Farrell, N. (2002) A comparison of DNA binding profiles of dinuclear platinum compounds with polyamine linkers and the trinuclear platinum phase II clinical agent BBR3464, *J. Biol. Inorg. Chem.* 7, 397–404.
17. Hegmans, A., Berners-Price, S. J., Davies, M. S., Thomas, D. S., Humphreys, A. S., and Farrell, N. (2004) Long range 1,4 and 1,6-interstrand cross-links formed by a trinuclear platinum complex. Minor groove preassociation affects kinetics and mechanism of cross-link formation as well as adduct structure, *J. Am. Chem. Soc.* 126, 2166–2180.
18. Berners-Price, S. J., Davies, M. S., Cox, J. W., Thomas, D. S., and Farrell, N. (2003) Competitive reactions of interstrand and intrastrand DNA-Pt adducts: A dinuclear-platinum complex preferentially forms a 1,4-interstrand cross-link rather than a 1,2-intrastrand cross-link on binding to a GG 14-mer duplex, *Chem. — Eur. J.* 9, 713–725.
19. Brabec, V., Kasparkova, J., Vrana, O., Novakova, O., Cox, J., Qu, Y., and Farrell, N. (1999) Effect of geometric isomerism in dinuclear platinum antitumor complexes on DNA interstrand cross-linking, *Biochemistry* 38, 10997–11005.
20. Harris, A., Qu, Y., and Farrell, N. (2005) Unique cooperative binding interaction observed between a minor groove binding Pt antitumor agent and hoeschst dye 33258, *Inorg. Chem.* 44, 1196–1198.
21. Qu, Y., Harris, A., Hegmans, A., Petz, A., Penazova, H., and Farrell, N. (2004) Synthesis and DNA conformational changes of non-covalent polynuclear platinum complexes, *J. Inorg. Biochem.* 98, 1591–1598.
22. Harris, A. L., Ryan, J. J., and Farrell, N. (2005) Biological consequences of trinuclear platinum complexes: Comparison of BBR 3464 to its non-covalent congeners, *Mol. Pharmacol.* (in press).
23. Bach, D. (1984) in *Biomembrane structure and function: Topics in molecular and structural biology* (Weinkeim, V., and Chapman, D., Eds.) pp 1–41, Verlag, Berlin, Germany.
24. Jain, M. K., and Wu, N. M. (1977) Effect of small molecules on dipalmitoyl lecithin liposomal bilayer. III. Phase-transition in lipid bilayer, *J. Membr. Biol.* 43, 157–201.
25. Tritton, T. R., Murphree, S. A., and Sartorelli, A. C. (1977) Characterization of drug-membrane interactions using liposome system, *Biochem. Pharmacol.* 26, 2319–2323.
26. Grenier, G., Berube, G., and Gioquaud, C. (1998) Effects of new triphenylethylene platinum(II) complexes on the interaction with phosphatidylcholine liposomes, *Chem. Pharm. Bull.* 9, 1480–1483.
27. Burger, K. N., Staffhorst, R. W., and De Kruijff, B. (1999) Interaction of the anti-cancer drug cisplatin with phosphatidylserine in intact and semi-intact cells, *Biochim. Biophys. Acta* 1419, 43–54.
28. Speelmans, G., Staffhorst, R. H. M., Versluis, K., Reedijk, J., and De Kruijff, B. (1997) Cisplatin complexes with phosphatidylserine in membranes, *Biochemistry* 36, 10545–10550.
29. Speelmans, G., Sip, W. H. H. M., Grisel, R. J. H., Staffhorst, R. H. M., Fichtinger-Schepman, A. M. J., Reedijk, J., and De Kruijff, B. (1996) The interaction of the anti-cancer drug cisplatin with phospholipids is specific for negatively charged phospholipids and takes place at low chloride ion concentration, *Biochim. Biophys. Acta* 1283, 60–66.
30. Farrell, N. (2004) Polynuclear Platinum Drugs, *Metal Ions Biol. Syst.* 41, 252–296.
31. Rauter, H., DiDomenico, R., Menta, E., Oliva, A., Qu, Y., and Farrell, N. (1997) Selective platination of biologically relevant polyamines. Linear coordinating spermidine and spermine as amplifying linkers in dinuclear platinum complexes, *Inorg. Chem.* 36, 3919–3927.
32. Bligh, E. G., and Dyer, W. L. (1959) A rapid method of total lipid extraction and purification, *Can. J. Biochem. Physiol.* 37, 911–917.
33. Blume, A. (1991) Biological calorimetry: Membranes, *Thermochim. Acta* 193, 299–347.
34. Zhang, J., Thomas, D. S., Davies, M. S., Berners-Price, S. J., and Farrell, N. (2005) Effects of geometric isomerism in dinuclear platinum antitumor complexes on aqutation reactions in the presence of perchlorate, acetate and phosphate, *J. Biol. Inorg. Chem.* 10, 652–666.
35. Bose, R. N., Goswami, N., and Moghaddas, S. (1990) Phosphato complexes of platinum(II): P-31 NMR and kinetics of formation and isomerization studies, *Inorg. Chem.* 29, 3461–3467.
36. Davies, M. S., Thomas, D. S., Hegmans, A., Berners-Price, S. J., and Farrell, N. (2002) Kinetic and equilibria studies of the aqutation of the trinuclear platinum phase II anticancer agent  $[\{\text{trans-PtCl}(\text{NH}_3)_2\}_2\{\mu\text{-trans-Pt}(\text{NH}_3)_2(\text{NH}_2(\text{CH}_2)_6\text{NH}_2)_2\}]^{4+}$  (BBR3464), *Inorg. Chem.* 41, 1101–1109.
37. Davies, M. S., Berners-Price, S. J., Cox, J. W., and Farrell, N. (2003) The nature of the DNA template (single-stranded versus double-stranded) affects the rate of aqutation of a dinuclear Pt anticancer drug, *J. Chem. Soc., Chem. Commun.* 1, 122–123.
38. Hermann, T., and Hansjorg, E. (1974) Electrostatic effects on lipid phase transitions: Membrane structure and ionic environment, *Proc. Natl. Acad. Sci. U.S.A.* 71, 214–219.
39. Ramaswami, V., Haaseth, R. C., Matsunaga, T. O., Hruby, V. J., and O'Brien, D. F. (1992) Opioid peptide interactions with lipid bilayer membranes, *Biochim. Biophys. Acta* 1109, 195–203.
40. Berridge, M. J. (1987) Inositol trisphosphate and diacylglycerol: 2 interacting 2nd messengers, *Annu. Rev. Biochem.* 56, 159–193.
41. Somermeyer, M. G., Knauss, T. C., Weinberg, J. M., and Hummes, H. D. (1983) Characterization of  $\text{Ca}^{2+}$  transport in rat renal brush-border membranes and its modulation by phosphatidic acid, *Biochem. J.* 214, 37–46.
42. Nishizuka, Y. (1986) Studies and perspectives of protein kinase C, *Science* 233, 305–312.



43. Anderson, L., Cummings, J., Bradshaw, Y., and Smyth, J. F. (1991) The role of protein-kinase-C and the phosphatidylinositol cycle in multidrug resistance in human ovarian-cancer cell, *Biochem. Pharmacol.* **42**, 1427–1432.
44. Rando, R. R. (1998) Regulation of protein kinase-C activity by lipids, *FASEB J.* **2**, 2348–2355.
45. Huang, Z., Tong, Y., Wang, J., and Huang, Y. (2003) NMR studies of the relationship between the changes of membrane lipids and the cisplatin-resistance of A549/DDP cells, *Cancer Cell Int.* **3**, 5.

BI052517Z